Impurity effects on domain-growth kinetics. II. Potts model

David J. Srolovitz
Los Alamos National Laboratory, Los Alamos, New Mexico 87545

Gary S. Grest
Corporate Research Science Laboratory, Exxon Research and Engineering Company, Annandale, New Jersey 08801
(Received 3 April 1985)

The development of order for the Q-state Potts model for $2<Q\leq 48$ in the presence of static, random impurities is studied following a quench from high temperature ($T\gg T_c$) to very low temperatures. We find that the domain growth becomes pinned for quenches to $T=0$ and the average pinned domain area A_f varies inversely with the concentration c of impurities. This value of the proportionality factor between A_f and c^{-1} can be understood in terms of a simple topological analysis for large Q.

I. INTRODUCTION

The kinetics of Potts model without impurities quenched from a high temperature T, far above the critical temperature T_c to a final temperature less than T_c, has recently been studied.[1,2] The mean linear domain size R was found to increase with time t as $R\approx t^n$. On a triangular lattice, n was found to be temperature independent for all $T<T_c$.[1] It did, however, depend on the degeneracy Q of the Potts model. In the limit that Q approached the Ising value ($Q=2$), n tended toward $\frac{1}{2}$, while for large Q, n saturated at $\sim 0.41\pm 0.02$.[1] The growth exponent on the square lattice appeared to be a function of T, being equal to zero for $T=0$ and rising to a value nearly equal to the growth exponent n on the triangular lattice by $T\approx T_c/2$.

The presence of quenched impurities is known to have important effects in experimental studies of domain growth. Quenched impurities can occur in many different forms; for example, second-phase particles in grain growth in polycrystalline materials[3] and/or surface defects in the ordering of atoms physisorbed on solid surfaces or intercalated into graphite.[4] As a routine matter, second-phase particles are added to metals and ceramics to control grain size. In these cases the final grain size is affected by both the particle concentration and size.[3]

In the preceding paper we reported the effect of quenched impurities on the kinetics of domain growth in a nonconserved Ising model.[5] Here, we generalize those results to the Q-state Potts model. Our interest in extending the Monte Carlo simulations to systems with many degenerate ground states comes from our earlier calculations[1] without impurities which showed that the kinetics of the Potts model is sensitive to changes in the degeneracy Q. That degeneracy manifests itself in the topology of the model. We will show that in the large-Q limit the topology of the model becomes a useful feature in predicting the effects of the quenched impurities. In this paper we report the results of studies in which Potts models on triangular lattices are quenched from $T\gg T_c$ to $T\cong 0$. The evolution of the models was controlled by nonconserved dynamics. The degeneracy Q was varied from $Q=3$ to 48 and the concentration of quenched impurities c from 0.5% to 20%. We find that in all cases studied, the domain growth becomes pinned for $T=0$ and the averaged pinned domain area varies inversely with the concentration of impurities.

II. PROCEDURE AND RESULTS

The Hamiltonian describing the Q-component ferromagnetic Potts model is written as

$$H=-J\sum_{\mathrm{NN}}\delta_{S_iS_j}\ , \tag{1}$$

where S_i is the Q state of the spin on site i ($1\leq S_i\leq Q$), δ_{AB} is the Kronecker δ function, and J is a positive constant. The summation in Eq. (1) is taken over all nearest-neighbor (NN) spins. Since, in the present simulations, the order parameter is nonconserved, spin-flip (or Glauber) dynamics is employed.[6] A more efficient Monte Carlo technique, known as the "n-fold" way, is employed to save computer time.[1]

The model was initialized by randomly placing Nc impurities with $S_i=0$ on the lattice, where N is the number of lattice sites and c is the concentration of quenched impurities. The remaining sites were assigned a random value between 1 and Q. During the course of the simulation the impurities were immovable and hence both the impurity positions and concentration were time independent. The impurities were noninteracting with each other or with spins on the occupied sites. Thus, the surface (line) energy of an impurity interacting with a spin on an occupied NN site is the same as the domain-boundary energy between two occupied sites with different orientations. We performed the simulations on a 200×200 triangular lattice for $Q>4$ and on a 400×400 triangular lattice for $Q=3$ and 4. For $Q<48$, results of ten configurations were averaged for each value of Q and c. For $Q=48$, five simulations were performed for $c\geq 0.02$ and two for smaller values of c, since much longer runs were necessary before the system became pinned.

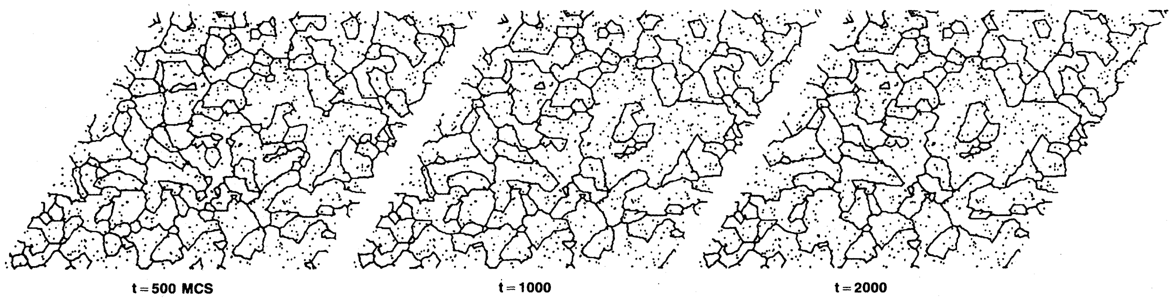

FIG. 1. Evolution of the domain-boundary configuration for the $Q=3$ Potts model quenched from $T \gg T_c$ to $T=0$ on a triangular lattice of size 400×400 with $c=0.01$.

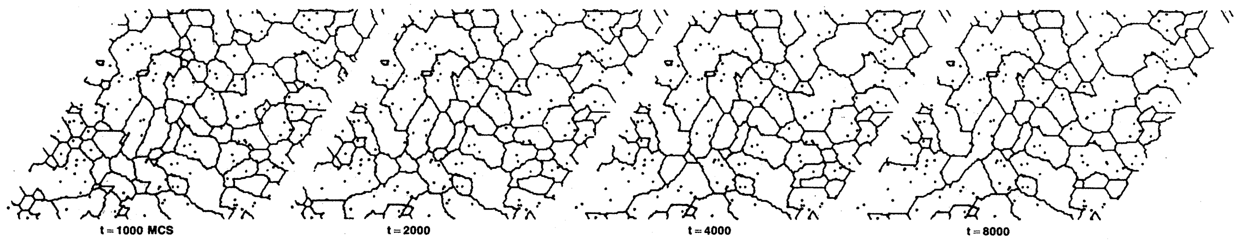

FIG. 2. Evolution of the domain-boundary configuration for the $Q=6$ Potts model quenched to $T=0$ on a triangular lattice of size 200×200 with $c=0.01$.

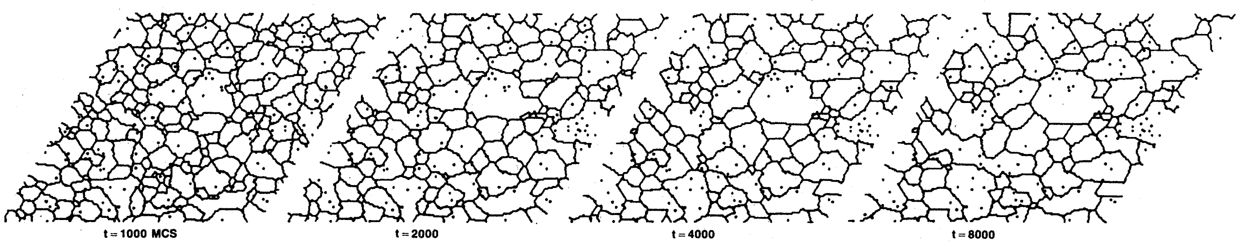

FIG. 3. Evolution of the domain-boundary configuration for the $Q=12$ Potts model quenched to $T=0$ on a triangular lattice of size 200×200 with $c=0.01$.

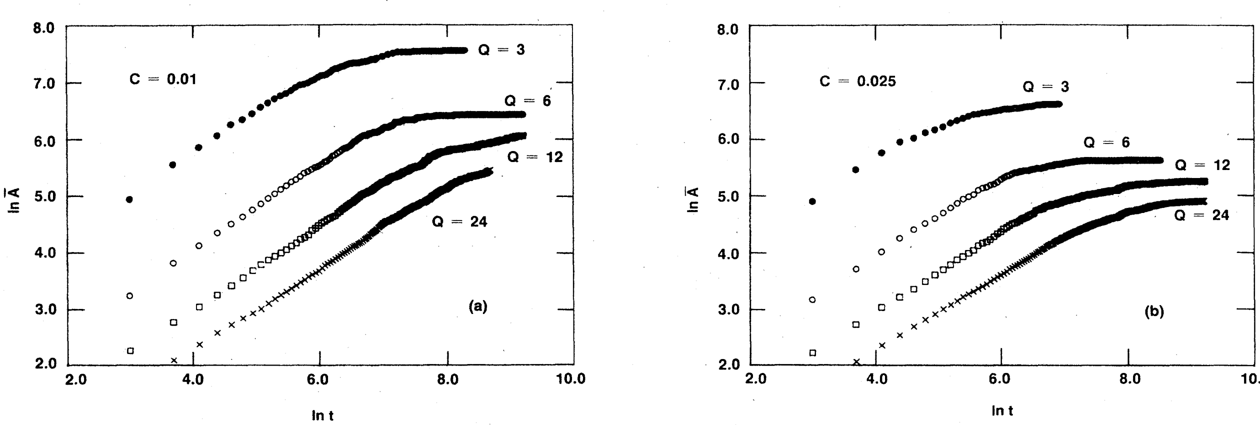

FIG. 4. Average domain area $\overline{A}$ plotted logarithmically vs the logarithm of time t for $Q=3$, 6, 12, and 24 for (a) $c=0.01$ and (b) $c=0.025$.

The temporal evolution of the microstructures are displayed in Figs. 1–3 for $Q=3$, 6, and 12, respectively, for $c=0.01$. Similar microstructures for $Q=48$ are given in Ref. 7. The solid lines separate domains of unlike spin orientation and the solid dots show the positions of the quenched impurities (plotted about twice their actual area). As in the domain growth without impurities, the domains become more compact with increasing Q. Examination of Figs. 1 and 2 shows that the time evolution of the microstructure is slowing down and ultimately becomes pinned by the last frame. Results for $Q=12$, Fig. 3, are not pinned by $t=8000$ MCS's, but do become pinned for much later times (MCS denotes Monte Carlo step per spin).

The evolution of the mean domain area with time is exhibited in Figs. 4 and 5. In Figs. 4(a) and 4(b) the effect of varying Q at fixed impurity concentration (1% and 2.5%, respectively) is shown. There it is seen that at early times the growth can be approximated by a power law $[\ln(A)\sim\ln(t)]$ crossing over at long times to much slower growth. For $T=0$ we believe the system is pinned for very long times. Increasing Q has the effect of decreasing the mean pinned domain size A_f, yet increasing the crossover time corresponding to the transition from power law to slow growth. The effects of varying the impurity concentrations at fixed Q are illustrated in Figs. 5(a) and 5(b) for $Q=4$ and 6, respectively. Both the final domain size

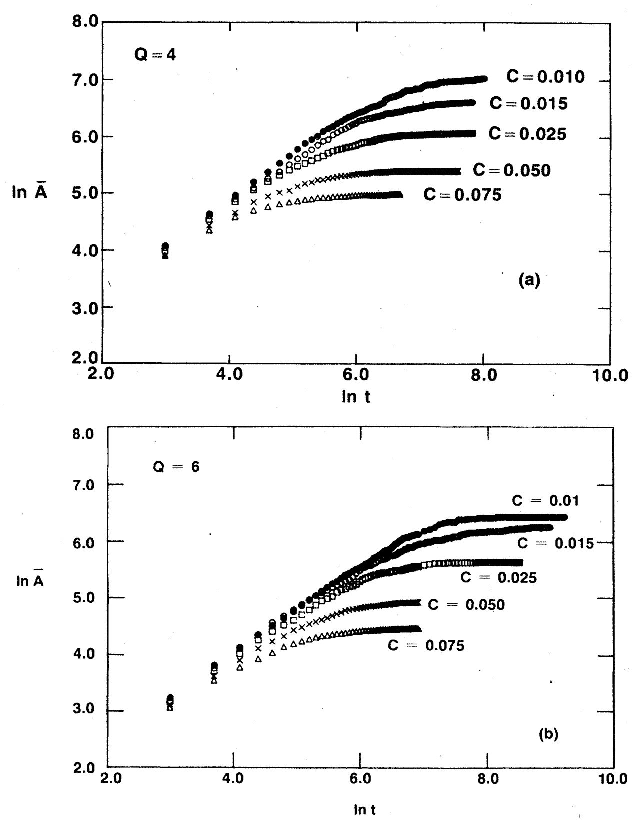

FIG. 5. Average domain area $\overline{A}$ plotted logarithmically vs the logarithm of time t for five concentrations c for (a) $Q=4$ and (b) $Q=6$.

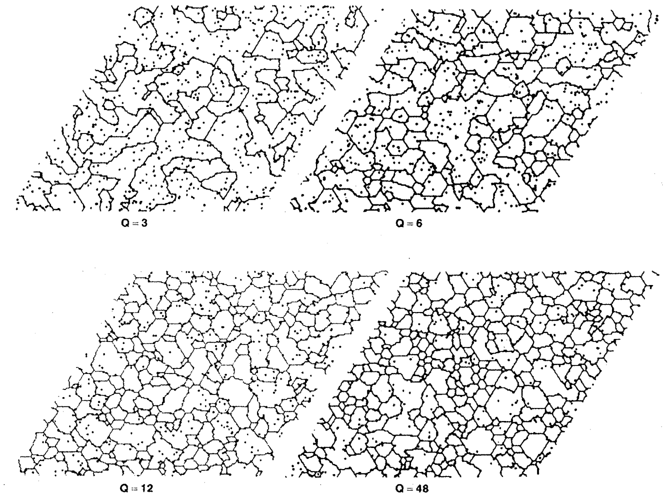

FIG. 6. Pinned microstructure for the Q-state Potts model quenched from $T \gg T_c$ to $T=0$ for four values of Q, with $c=0.025$ on a triangular lattice of size 200×200.

and time required for pinning increase with decreasing impurity concentration. Results for the energy $E(t)$ and the mean chord length[5] $\overline{L}(t)$ showed very similar results, but since the average area gives a more direct measure of the order in the system, we present results only for A, unlike in our preceding paper,[5] where for $Q=2$ the area was found not to be an appropriate measure.

As seen in Figs. 4 and 5, all models with nonzero impurity concentrations become pinned at sufficiently long times for $T=0$. Figure 6 shows some pinned configurations for different values of Q with $c=0.025$. The increase of A_f with decreasing Q, discussed in conjunction with Fig. 4, is easily seen in these configurations. The dependence of A_f on the impurity concentration is shown in Fig. 7 for five values of Q. These data indicate that A_f depends inversely on the impurity concentration. However, the proportionality factor relating A_f to $1/c$ is clearly dependent on the degeneracy of the model, Q. Least-squares fits to the slopes M of the curves in Fig. 7 indicate a trend of increasing proportionality constant with decreasing Q.

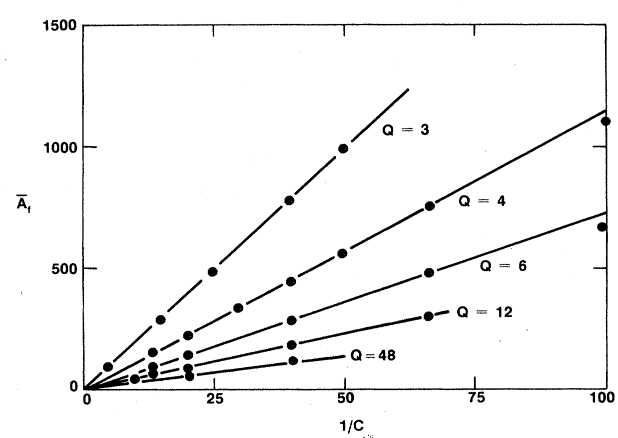

FIG. 7. Averaged pinned area A_f vs inverse concentration c^{-1} for several values of Q.

III. DISCUSSION

The data and the microstructures in Figs. 1–6 show that domain growth occurs readily at early times, but that the domain structure is pinned at late times. In the log-log plots of Figs. 4 and 5 it is seen that the transition between these two regimes is relatively sharp (on a logarithmic timescale). At early times the data may be interpreted as indicating power-law growth. However, care must be exercised in extracting the growth exponent when the power-law regime is not sufficiently far removed from the influences of the particle pinning. This crossover from power-law growth to pinning occurs at later times with increasing Q and/or decreasing impurity concentration. While no data are presented here on the temperature dependence of domain growth in the presence of impurities, our Ising results[5] show that the transition also occurs at later times with increasing temperature. The role of temperature is to provide the thermal fluctuations necessary for the domain boundary to bypass the quenched impurities.

From our large-Q simulations we can extract domain-growth exponents within the power-law regime which are consistent with our results for $c=0$. For $Q=48$ we found[7] $n=0.39\pm0.02$ ($\overline{R}\sim t^n$). This value is in agreement with the growth exponents observed in our impurity-free simulations.[1] However, for small values of Q we always measured smaller effective exponents for the early-time regime compared to our estimates for $c=0$. For the smallest impurity concentrations used here ($c=0.005$), the crossover from a power-law regime to a logarithmic or pinned regime was still not out far enough to obtain an estimate of n independent of c for small Q. Our results for large Q suggest that the early-time regime of domain growth in the presence of impurities is much like that of normal (no impurities) domain growth as long as the average domain size R is small compared to the average impurity spacing. In this way the early-time regime may be thought of as representative of an ensemble of small growing regions.

Domain growth stops when the domain size is comparable with the interimpurity spacing. While the concept of comparing domain size with interimpurity spacing is well defined when the domains are compact, the domains become increasingly less compact[8] with decreasing Q (see Figs. 1–3). For the Ising model the length scale of the domains is not adequately described by the square root of the domain area and a correlation length calculated via the mean perimeter, chord length, or structure factor is more meaningful.[5] Since domain boundaries are effectively pinned by impurities, the slope M of the A_f-versus-$1/c$ plots (Fig. 7) or, equivalently, cA_f, provides a measure of the compactness of the domains. The slopes in Fig. 7 range from approximately 3 at $Q=48$ to 20 at $Q=3$. In the Ising limit $Q=2$, we find[5] that $cA_f=c\pi R_f^2$ is approximately 50 or 65 depending on whether R_f is equated with the mean chord length $\overline{L}$ or the perimeter $\overline{R}$, respectively. The slopes change more slowly with Q for large Q than they do for small Q. This is consistent with our observations on the impurity-free simulations where we found that the kinetics, topology, and domain-size distribution saturate for large Q.[1] The value of M at which the data saturate may be understood with the aid of a simple topological argument.[7] Since domain growth occurs when small domains are annihilated and domain annihilation occurs by the meeting of three domain vertices, domain growth stops when domain vertices can no longer meet. Motion of vertices is prevented when the three domain boundaries meeting at the vertex are pinned. Therefore, in two dimensions, where the mean number of edges (or vertices) per domain is six (Euler relation), the average number of impurities needed per domain is three: six edges per domain divided by two to account for the fact that each edge is shared by two domains. A more complete topological analysis may be found in Ref. 7 for $Q=48$.

In order to determine the nature of the Q dependence of the slope M in the plot of A_f versus $1/c$ (Fig. 7), we make use of two observations. First, as noted above, M tends to three as Q goes to infinity. Second, since M is undefined for $Q=1$ (single domain), Q should be normalized as $Q-1$. In Fig. 8 we plot $\ln(M-3)$ versus $\ln(Q-1)$. Within the statistics of the simulation, we find that

$$M=A_fc=3+B(Q-1)^{-1.5}, \quad (2)$$

where $B=48.7\pm2.9$ and the statistical error on the exponent is ±0.1. Equation (2) collapses all of our data on the interplay of final domain size, impurity concentration, and degeneracy onto one curve. Although the Ising ($Q=2$) results were not included in Fig. 8, they are also well described by Eq. (2).

In summary, we have studied domain growth in the nonconserved Potts model with quenched impurities. The mean domain area is initially found to increase with time as a power law. For sufficiently large times, the domain

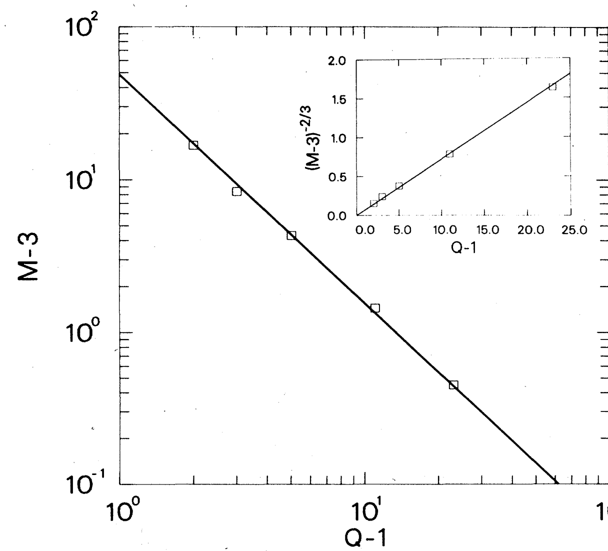

FIG. 8. Logarithm of $M-3=A_fc-3$ is plotted vs $\ln(Q-1)$. Inset: linear plot of $(M-3)^{-2/3}$ vs $Q-1$, where the exponent has been extracted from the main plot. The solid line is taken from Eq. (2).

growth slows to logarithmic or pins for quenches to $T=0$. The final domain area is proportional to the inverse of the impurity concentration. The proportionality constant decreases with increasing Q and is asymptotic to 3 as Q tends toward infinity. The value of this constant for large Q can be rationalized in terms of a simple topological analysis.

ACKNOWLEDGMENT

The authors gratefully acknowledge the hospitality of the Institute for Theoretical Physics, University of California, Santa Barbara, where part of this paper was written.

[1]P. S. Sahni, G. S. Grest, M. P. Anderson, and D. J. Srolovitz, Phys. Rev. Lett. **50**, 263 (1983); P. S. Sahni, D. J. Srolovitz, G. S. Grest, M. P. Anderson, and S. A. Safran, Phys. Rev. B **28**, 2705 (1983).

[2]K. Kaski, J. Nieminem, and J. D. Gunton, Phys. Rev. B **31**, 2998 (1985); J. Viñals and J. D. Gunton (unpublished).

[3]P. A. Beck, M. L. Holzwarth, and P. Sperry, Trans. AIME **180**, 163 (1949).

[4]H. Homma and R. Clarke, Phys. Rev. Lett. **52**, 629 (1984).

[5]G. S. Grest and D. J. Srolovitz, preceding paper [Phys. Rev. B **32**, 3014 (1985)].

[6]R. J. Glauber, J. Math. Phys. **4**, 294 (1963).

[7]D. J. Srolovitz, M. P. Anderson, G. S. Grest, and P. S. Sahni, Acta Metall. **32**, 1429 (1984).

[8]G. S. Grest and D. J. Srolovitz, Phys. Rev. B **30**, 5150 (1984).